Eur. Phys. J. D **43**, 85–89 (2007)
DOI: 10.1140/epjd/e2007-00116-7

THE EUROPEAN PHYSICAL JOURNAL D

# Threshold laws in delayed emission: an experimental approach

B. Climen, F. Pagliarulo, A. Ollagnier, B. Baguenard, B. Concina, M.A. Lebeault, F. Lépine, and C. Bordas[a]

Laboratoire de Spectrométrie Ionique et Moléculaire, UMR CNRS 5579, Université Lyon 1, 69622 Villeurbanne, France

Received 18 August 2006 / Received in final form 16 October 2006
Published online 24 May 2007 – 

**Abstract.** Delayed emission is a common decay process for very excited complex systems where the excitation energy is, to a large extent, statistically distributed over all accessible degrees of freedom. A rich variety of delayed decay processes is found in complex molecules and clusters such as thermionic emission, evaporation of heavy fragments or blackbody radiation. In this article, we present the general threshold laws that govern the kinetic energy spectrum of matter particles (electrons or fragments) ejected from spherically symmetric species in such processes, and we illustrate these laws by experimental results obtained in photoelectron and photoion spectroscopy. Deviations from simple laws for non spherical species are also evidenced.

**PACS.** 36.40.-c Atomic and molecular clusters – 36.40.Qv Stability and fragmentation of clusters – 33.60.Cv Ultraviolet and vacuum ultraviolet photoelectron spectra

## 1 Introduction

Optical excitation in the visible or near-UV range of clusters and complex molecules results primarily in an electronic excitation and the major part of the internal energy is initially deposited in the electronic modes. If the photon energy is not large enough to bring the system into the ionization continuum, and if the photon absorption rate is much smaller than the internal couplings, the excitation energy is redistributed among the various internal degrees of freedom of the system. In case of a long pulse excitation, the system may subsequently absorb several photons with, after each step, a complete redistribution of the energy. Therefore, by multiphoton excitation, a complex system may be substantially heated following an optical excitation. Very often, even if the photon energy is large enough to ionize (or detach) the system, the very strong couplings between nuclear and electronic degrees of freedom result in a quasi-statistical redistribution of the internal energy over a timescale short enough to compete efficiently with direct emission. Therefore, as well in one-photon excitation as in multiphoton excitation processes, delayed emission [1] is a major decay channel for clusters and large molecules.

The theoretical description of such processes relies first on the assumption of a statistical equilibrium. Within this assumption, several approaches have been followed like the Weisskopf formulation of the detailed balance theory [2], the RRKM method [3] or the phase-space theory [4]. Only the degree and the nature of the approximations differ among these theories [5]. In the present article, we will follow the detailed balance theory [2,6,7], however similar results are obtained with the other descriptions [3,4,8,9]. The hypothesis of statistical redistribution of the internal energy is relatively well sustained in systems having a large number of degrees of freedom combined with large electron — vibration couplings such as large metal clusters or fullerenes. This assumption is markedly less obvious in smaller systems (typically around 10 atoms) and only a critical comparison between model and experimental results may ensure the validity of this hypothesis.

## 2 General description of decay from finite-size systems

Let us assume a finite-size system, designated as the parent, decaying by ejection of a particle and release of energy into final products following the generic path:

$$\text{parent} \rightarrow \text{ daughter } + \text{ ejected particle.} \qquad (1)$$

Decay occurs only if the parent system has an internal energy larger than the binding energy of the ejected particle in reaction (1). According to the magnitude of the various decay rates and depending on the relative binding energies, the ejected particle may either be a photon (blackbody radiation), an electron (thermionic emission), or a heavy fragment (evaporation). The global evolution of the system is driven by the integrated decay rates that determine the relevant timescales and the dynamics of the decay. However, a refined understanding of the ongoing processes requires in addition the knowledge of the differential decay rates. In the present article we focus on the general evolution of these differential decay rates as a function of the kinetic energy $\varepsilon$ released in the reaction.

[a] e-mail: bordas@lasim.univ-lyon1.fr

We therefore will consider only emission of matter particles: electron or fragments.

As stated above, we will follow the general approach of the detailed balance theory [2,6,7] which allows factoring the differential decay rate explicitly in terms expressing the degree of excitation of the system on one hand, and terms describing the interaction among final products on the other hand. Neglecting the internal degrees of freedom of the ejected particle the differential decay rate may be expressed as follows:

$$k_{decay}\left(E,\varepsilon\right)=\frac{gm}{\pi^2\hbar^3}\,\sigma(\varepsilon)\,\varepsilon\exp\left[-\frac{E_b}{k_BT_e}\right]\exp\left[-\frac{\varepsilon}{k_BT_d}\right] \tag{2}$$

where $E_b$ is the binding energy of the ejected particle, $T_d$ is the daughter temperature (temperature of the daughter system of internal energy $E-E_b$), $T_e$ is the emission temperature (temperature of a system of internal energy $E-E_b/2$) and $\sigma(\varepsilon)$ is the capture cross-section for the reverse process. The constants $g$, $m$ and $k_B$ are respectively the spin degeneracy, the mass of the ejected particle and the Boltzmann constant. By integration over the kinetic energy variable $\varepsilon$ one obtains an expression for the total decay rates. The present work however precisely does not deal with integrated rates. Rather, we are able to access experimentally the variation with $\varepsilon$ of the differential emission rate owing to the specific advantages of imaging techniques at threshold. As far as the variation of the differential emission rate as a function of $\varepsilon$ is concerned, it is proportional to

$$k_{decay}\left(E,\varepsilon\right)\propto\sigma(\varepsilon)\,\varepsilon\exp\left[-\frac{\varepsilon}{k_BT_d}\right] \tag{3}$$

where the capture cross-section $\sigma(\varepsilon)$ describes an intrinsic property of the system, while the term $\exp\left(-\varepsilon/k_BT_d\right)$ may be seen as a thermometer of the excited species. Under appropriate approximations, the capture cross-section may be related rather simply to the interacting potential between the ejected particle and the remaining system. The most trivial situation is found for bulk matter. In this limit, the capture cross-section does not vary with the kinetic energy and equation (3) reduces to:

$$k_{decay}\left(E,\varepsilon\right)\propto\varepsilon\exp\left[-\frac{\varepsilon}{k_BT_d}\right]. \tag{4}$$

For finite size systems, rather general forms may be derived as soon as spherical symmetry is assumed. In the spherical symmetry approximation the interacting potential at a distance $r$ from the center of the cluster may be, at first order, expressed as:

$$V\left(r\right)=-\frac{C_p}{r^p} \tag{5}$$

for $r>R_n$, where $R_n$ is the radius of the cluster; and $V(r)\to\infty$ for $r\leqslant R_n$ (hard-sphere approximation). The exponent $p$ corresponds to the nature of interaction, while $C_p$ is a constant describing the strength of the interaction. Under this approximation, it may be shown very generally [9,10] that in the limit of small $R_n$ and $\varepsilon$ values the capture cross-section is proportional to $\varepsilon^{\gamma-1}$ where

$$\gamma=\frac{p-2}{p}. \tag{6}$$

Leading to the following form of the differential decay rate:

$$k_{decay}\left(\varepsilon\right)\propto\varepsilon^{\gamma}\exp\left(-\frac{\varepsilon}{k_BT_d}\right). \tag{7}$$

Note that this expression is a first order development in $\varepsilon$. As such, it is exact only for small $\varepsilon$ values, i.e. just above threshold, hence the term threshold law. This simple formula allows deriving generic threshold emission laws for various processes governed by simple interacting potentials that correspond to realistic experimental situations as we will show in the section below. In the case of delayed ionization [11] for instance, Coulomb interaction prevails between the products and $\gamma=0$ while in the case of delayed detachment [12] the interacting potential, between a point charge and a polarizable core, is well represented by a Langevin potential ($p=4$) and the exponent is $\gamma=1/2$. In the case of delayed emission of heavy fragment (evaporation) [13], the situation also depends on the charge state of the fragments. When a singly charged ion cluster dissociates, one of the two fragments is generally neutral while the other fragment is charged. The situation is comparable to the case of detachment and the interaction between a charged species and a polarizable one is described by a Langevin potential and the exponent is $\gamma=1/2$. By contrast, when dissociation of a neutral cluster leads to the ejection of two neutral fragments the van der Waals interaction potential ($p=6$) between the two neutral systems implies $\gamma=2/3$. These threshold laws are illustrated by experimental examples below.

## 3 Experimental set-up

The experimental set-up used to study delayed emission of small clusters relies essentially on a versatile laser vaporization source for the production of free clusters and time-resolved photoelectron or photoion imaging [14]. Small anion clusters are produced by laser ablation. Native anions are extracted using a pulsed electric field in the extraction region of a time-of-flight mass-spectrometer. Clusters of specific mass, selected by their time-of-flight, are then excited by a second laser beam (Xe:Cl, 308 nm, pulse duration 15 ns, or Xe:Cl pumped dye laser) above their photodetachment threshold in the center of the interaction region of the photoelectron imaging spectrometer. The excitation of a well-defined cluster mass is ensured by firing the excitation laser when the given size is at the center of the electron spectrometer. In the case of neutral species like $C_{60}$, a pure molecular beam is obtained by laser desorption, or by evaporation in a thermal oven. In that case, multiphoton excitation is achieved in the center of the imaging spectrometer and, thanks to the slow velocity of

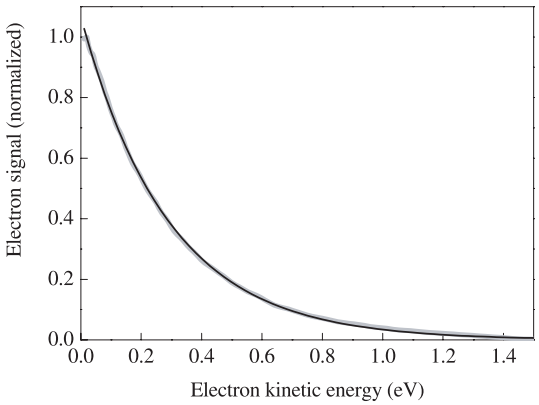


**Fig. 1.** Photoelectron spectrum (bold grey line) recorded in multiphoton delayed ionization of $C_{60}$ excited at $\lambda = 355$ nm. Only electrons ejected in the time window 250–350 ns after excitation are detected. An excellent agreement with an exponential profile ($\gamma = 0$, thin black line) leads to an experimental temperature $T_d = 3370 \pm 100$ K.

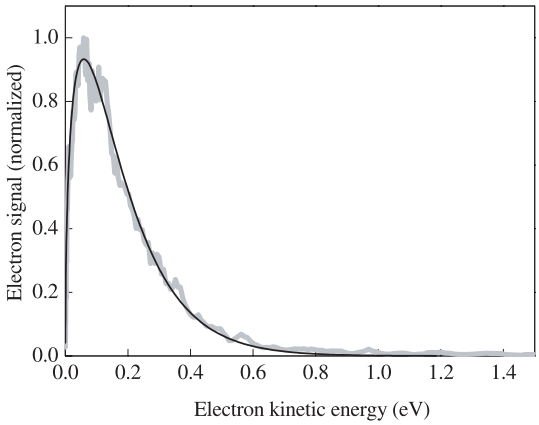


**Fig. 2.** Photoelectron spectrum (bold line) recorded in one-photon delayed detachment of $C_{20}^-$ at $\lambda = 308$ nm in the time window 60–120 ns after excitation. A fit to equation (7) with $\gamma = 1/2$ (thin line) gives $T_d = 1376 \pm 50$ K.

the neutral beam, electrons as well as ion fragments may be analyzed and their kinetic energy measured. The imaging spectrometer itself is strictly identical for electron or positive ions, except for the reverse polarities. The principle of charged particle imaging introduced in the early 80's [15] is extremely simple. A static electric field is applied in the interaction region and used to project the charged particles onto a position sensitive detector (PSD) made up of a tandem microchannel plates followed by a phosphor screen and a CCD camera. Our set-up uses the principle of velocity-map imaging [16]. The electrodes of the spectrometer and the applied voltages are designed such that the resulting extraction field projects the electrons or ions onto the PSD with a position of impact depending only on the initial velocity, irrespective of the initial position. By summing particle impacts over many laser shots one obtains a map of the projection of the initial velocity on a plane perpendicular to the electric field. A standard inversion method [14,17] allows the extraction of angle resolved kinetic energy distribution. Imaging relies entirely on geometrical properties of the particle trajectories to measure the kinetic energy. Therefore, since the dispersion in time of flight for a given species is negligible, this method is intrinsically capable of time-resolution. By simply gating the microchannel plates [18], one can select a given time slice in the electron distribution and then record a delayed electron emission spectrum in a well defined time window after excitation. Alternatively, we can selectively detect a well defined ion mass, allowing to record mass selected ion KER distributions. The modest time resolution of our system (about 60 ns) is however appropriate to the timescale of the observed phenomena.

## 4 Experimental results

Let us now illustrate the threshold laws introduced above by some selected examples obtained in delayed emission of small excited carbon or metal clusters. Let us first start with delayed ionization of a neutral system. Figure 1 presents a typical electron spectrum recorded in multiphoton ionization of $C_{60}$ [19,20] in the near UV (355 nm, 10 ns pulse duration) in a time window between 250 and 350 ns after excitation. Owing to its high symmetry, the fullerene $C_{60}$ is assumed to be rather well described by the approximations described in Section 2, especially regarding the spherical symmetry. Indeed, the agreement between a simple exponential form ($\gamma = 0$) and the experimental kinetic energy distribution is extremely good and allows to derive a daughter temperature of about 3400 K. The exponential profile, characteristic of ionization, has been found at every delay between 50 ns and more than 10 $\mu$s. Note that in this case, the multiphoton excitation process leads to a broad internal energy distribution. As shown in [20], a given observation window corresponds therefore to a narrow slice in the internal energy distribution, i.e. to a rather well-defined microcanonical ensemble. In the case of $C_{60}$, the time resolution allows measuring the decrease of $T_d$ as a function of time delay after excitation, giving a direct access to the total decay rate.

In the case of delayed photodetachment the kinetic energy distribution is significantly different and the $\gamma$ parameter is expected to be 1/2. This has been observed indeed in one-photon detachment of carbon [21,22] or tungsten [23,24] anion clusters as shown in Figures 2 and 3. In these cases, the best agreement between the delayed electron spectrum and equation (7) is found, as expected, with $\gamma = 1/2$. These results show that the differential emission rate in delayed electron emission varies consistently along the lines described above both in case of ionization of neutrals of in case of detachment of anions. Note that, while $C_{60}$ or small tungsten clusters are reasonably well described by spherical symmetry this is not the case for small carbon anions like $C_{20}^-$ which most stable isomer is a monocyclic ring. Like in the case of $C_{60}$ delayed ionization, the internal energy distribution is broad, but

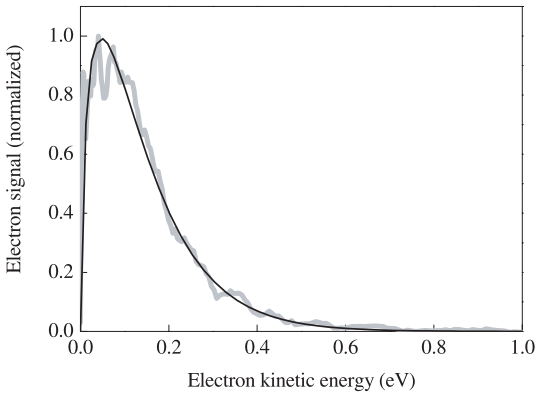


**Fig. 3.** Same as Figure 2 in the case of $W_{10}^-$. A fit with $\gamma = 1/2$ (thin line) gives $T_d = 1097 \pm 50$ K.

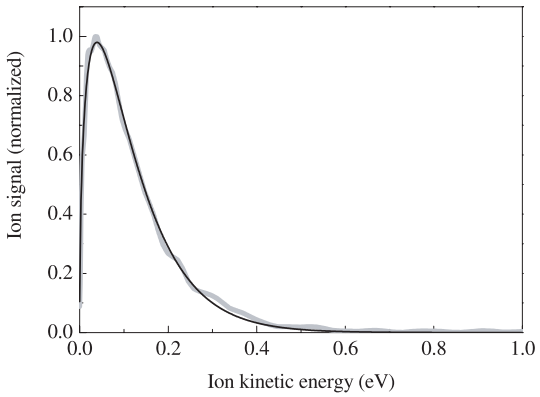


**Fig. 4.** Kinetic energy spectrum (bold grey line) of $C_{48}^+$ fragments ejected in multiphoton ionization of $C_{60}$ at 355 nm (nanosecond regime). The experimental curve is fitted using a free $\gamma$ parameter. Best fit is found for $\gamma = 0.49 \pm 0.05$ (thin line). The average kinetic energy in the lab frame is $\bar{\varepsilon} = 119 \pm 10$ meV.

mainly owing to the loose control of the internal degree of excitation during the production process.

In the case of evaporation the situation is slightly more difficult to evaluate in the sense that in most frequent cases evaporation results in the production of two neutral fragments while only charged fragments are measured in our set-up. The case of $C_{60}$ offers a situation where ion fragments are ejected and may be analyzed following our procedure. However, the emission of charged fragments $C_{60-2n}^+$ results from a chain of fragmentation where fullerenes decay by ejecting one electron and one or several $C_2$ fragments (the ionization step being generally the last one). Therefore, fragmentation is a mixture of two different processes, one characterized by an exponent 1/2 (ion), the other one by an exponent 2/3 (neutral). This means that the distinction between threshold laws relevant to neutrals or ions cannot be made explicitly in the present case. Practically, as shown in Figure 4 with the typical example of $C_{48}^+$, the kinetic energy distribution of photoions is best fitted using a parameter $\gamma$ close to 1/2. This tends to show that the step corresponding to the ejection of an ion fragment prevails, however only a detailed analysis of the fragmentation chain may answer this question unambiguously. In this case, our experimental results are compatible with the model described in chapter 2, but do not allow distinguishing between ejections of neutral or charged fragments.

All experimental results presented so far confirm the assumptions made in Section 2. The question now arises of the influence of the geometry for a system departing largely from spherical symmetry like for instance a linear carbon chain. Figure 5 shows a typical example of a photoelectron spectrum recorded in delayed detachment of $C_{10}^-$ [25]. As opposed to larger carbon anion clusters, the emission spectrum of this linear molecule does not present the same behavior and a fit with equation (7) using a free exponent parameter leads to a much smaller value $\gamma \approx 0.2$. All spectra recorded at various wavelengths and for other small linear carbon anion clusters with less than 12 atoms exhibit a small value of the parameter $\gamma$, typically around 1/4. This result indicates unambiguously that in the case of a large departure from spherical symmetry the threshold laws for emission has to be modified accordingly in order to take into account both finite-size and different symmetry.

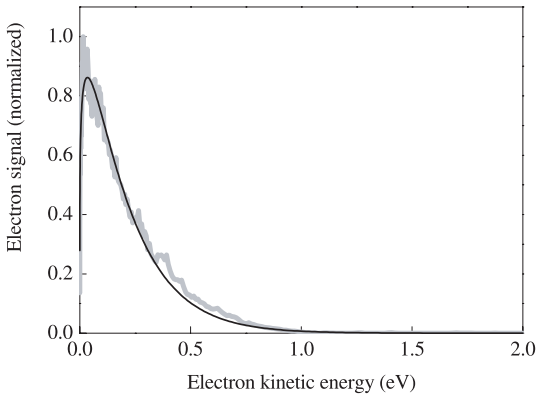


**Fig. 5.** Variable exponent adjustment for delayed spectrum obtained in the photodetachment of $C_{10}^-$. Bold line: experiment, thin line: fit. Best agreement is found with $\gamma = 0.20$ and $T_d = 2035 \pm 100$ K. The low value of $\gamma$ is suspected to arise from the non spherical symmetry of this small linear chain.

## 5 Conclusion

Our experimental results have allowed illustrating the threshold laws derived from the detailed balance theory for emission of charged particles from a more or less spherically symmetric cluster or molecule in the case of ionization or detachment, as well as in the case of evaporation of heavy fragment. These results also illustrate that the kinetic energy distribution of charged particles in delayed emission from small clusters obey in most cases rather universal threshold laws confirming simple forms of the threshold capture cross section. The energy spectrum provides also a universal thermometer characteristic of the fragment and of the timescale of observation.

Significant departures from these simple laws are found in recent results obtained on small linear carbon chains, i.e. for species that cannot be represented correctly by conducting sphere. Development of the model in order to account for ellipsoidal or cylindrical symmetry is presently under progress.

The "Laboratoire de Spectrométrie Ionique et Moléculaire" is a "Unité Mixte de Recherche CNRS-Université Lyon 1" (UMR CNRS 5579).

## References

1. E.E.B. Campbell, R.D. Levine, Annu. Rev. Phys. Chem. **51**, 65 (2000)
2. V. Weisskopf, Phys. Rev. **52**, 295 (1937)
3. O.K. Rice, H.C. Ramsperger, J. Amer. Chem. Soc. **49**, 1617 (1927); L.S. Kassel, J. Phys. Chem. **35**, 1065 (1928); R.A. Marcus, O.K. Rice, J. Phys. Coll. Chem. **55**, 894 (1951); R.A. Marcus, J. Chem. Phys. **20**, 359 (1952)
4. J.C. Light, Disc. Faraday Soc. **44**, 14 (1967); C.E. Klots, J. Phys. Chem. **75**, 1526 (1971); W.J. Chesnavitch, M.T. Bowers, J. Chem. Phys. **66**, 2306 (1977)
5. *Unimolecular reactions, a concise introduction*, edited by W. Forst (Cambridge University Press, 2003)
6. J.U. Andersen, C. Gottrup, K. Hansen, P. Hvelplund, M.O. Larsson, Eur. Phys. J. D **17**, 189 (2001)
7. J.U. Andersen, E. Bonderup, K. Hansen, J. Phys. B **35**, R1 (2002)
8. C.E. Klots, J. Chem. Phys. **100**, 1035 (1994)
9. C.E. Klots, J. Chem. Phys. **98**, 1110 (1993)
10. F. Calvo, P. Parneix, Comput. Mat. Sci. **35**, 198 (2006)
11. A. Amrein, R. Simpson, P. Hackett, J. Chem. Phys. **94**, 4663 (1991)
12. G. Ganteför, W. Eberhardt, H. Weidele, D. Kreisle, E. Recknagel, Phys. Rev. Lett. **77**, 4524 (1996)
13. K. Gluch, S. Matt-Leubner, O. Echt, B. Concina, P. Scheier, T.D. Märk, J. Chem. Phys. **121**, 2137 (2004)
14. *Imaging in Molecular Dynamics*, edited by B.J. Whitaker (Cambridge University Press, 2003)
15. D.W. Chandler, P.L. Houston, J. Chem. Phys. **87**, 1445 (1987)
16. A.T.J.B. Eppink, D.H. Parker, Rev. Sci. Instrum. **68**, 3477 (1997)
17. C. Bordas, F. Paulig, H. Helm, D.L. Huestis, Rev. Sci. Instrum. **67**, 2257 (1996)
18. B. Baguenard, J.B. Wills, F. Pagliarulo, F. Lépine, B. Climen, M. Barbaire, C. Clavier, M.A. Lebeault, C. Bordas, Rev. Sc. Instrum. **75**, 324 (2004)
19. F. Lépine, B. Climen, F. Pagliarulo, B. Baguenard, M.-A. Lebeault, C. Bordas, M. Hedén, Eur. Phys. J. D **24**, 393 (2003)
20. F. Lépine, C. Bordas, Phys. Rev. A **69**, 053201 (2004)
21. B. Baguenard, J.C. Pinaré, F. Lépine, C. Bordas, M. Broyer, Chem. Phys. Lett. **352**, 147 (2002)
22. J.B. Wills, F. Pagliarulo, B. Baguenard, F. Lépine, Ch. Bordas, Chem. Phys. Lett. **390**, 145 (2004)
23. J.C. Pinaré, B. Baguenard, C. Bordas, M. Broyer, Phys. Rev. Lett. **81**, 2225 (1998)
24. B. Baguenard, J.C. Pinaré, C. Bordas, M. Broyer, Phys. Rev. A **63**, 023204 (2001)
25. F. Pagliarulo, B. Climen, B. Baguenard, F. Lépine, M.A. Lebeault, A. Ollagnier, J. Wills, C. Bordas, Int. J. Mass Spectr. **252**, 100 (2006)